Article

High-Temperature Ash Melting and Fluidity Behavior upon the Cocombustion of Sewage Sludge and Coal

Yunpeng Yu, Zhiao Yu, Wei Xu, Kaibing Zhang, Yuneng Tang, Guojian Cheng, Xiang He, and Baiqian Dai*

Read Online

| ACCESS | | Metrics & More | | Article Recommendations |

ABSTRACT: Wastewater treatment produces a large amount of sludge, where the minimizing of the disposed sludge is essential for environmental protection. The co-combustion of sludge with coal is a preferable method for sewage sludge disposal from the economic and environmental perspective. The co-combustion of sludge has been widely used in the industry with the advantages of large processing capacity. The melting characteristics of ash are an important criterion for the selection of the co-combustion methods and furnace types. In this study, two types of sludge and four types of coal with different ash melting points were selected, where the ash melting behavior upon co-combustion is investigated by experimental and thermodynamical approaches. Especially, the slag fluidity upon co-combustion is explored via a modified inclined plane method. It has been found that the presence of SiO_2 and CaO in sludge substantially enhances its fusion temperature owing to the high content of CaO, while SiO_2 acts as a solvent, facilitating the co-melting of other oxides and raising the sludge fusion temperature. Fe_2O_3 exhibits a specific mass fraction within the range of 10−20%. Furthermore, the presence of CaO and SiO_2 prohibits the flow ability of the slag at high temperatures, and Fe_2O_3 promotes the flow ability for sludge at high temperatures. With increasing base/acid ratio, the sludge flow velocity increases remarkably and peaks at 1.6. The interaction between Fe−Ca and Si−Al significantly affects the fluidity significantly. The findings are expected to optimize the condition of co-combustion and desirable furnace design for the incineration of sludge.
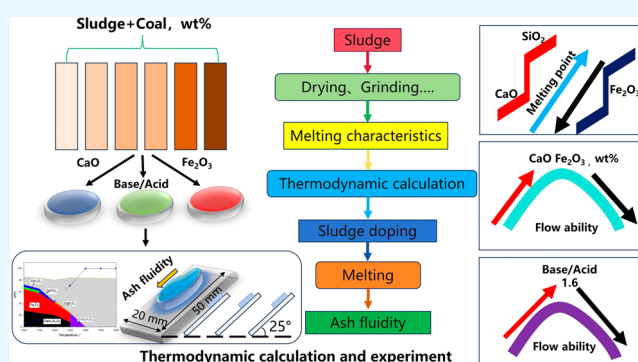
INTRODUCTION

With the development of the economy and the increase in urban population, the amounts of discharged industrial wastewater and untreated sludge are increasing. According to the EU report, more than 10 million tons of dry solids of sewage sludge was produced in 26 EU member states in 2008, of which approximately 36% (3.7 million tons of dry solid) was recycled in agriculture.[1] China's sludge production will reach 90 million tons per year in 2025.[2,3] The treatment of wastewater sludge is challenging because of its high moisture content and the presence of harmful substances.[4] It causes secondary pollution to waterbodies and the atmosphere; thus, improperly treated sludge poses a critical threat to the ecological environment and human health. Currently, the main sludge treatment methods include landfilling,[5] agricultural use, combustion,[6,7] and utilization as a raw material for manufacturing construction bricks.[8] Among these, the sludge combustion process has various advantages and is highly suitable for treating large amounts of excess sludge.[9,10] In addition, the energy produced via incineration can be used for power generation and heating. Nevertheless, the combustion of

sludge is hindered by its low calorific value,[11,12] necessitating the addition of auxiliary fuels. The co-combustion of sludge with coal has proven to be an effective method for enhancing sludge combustion[13] and reducing conventional pollutants and dioxin in flue gas emissions.[14] Furthermore, the volatilization of heavy metals during sludge combustion[15] is a secondary pollution issue associated with sewage sludge. Studies have found that the distribution of heavy metals in the ash during sludge combustion varied across different sampling positions,[16,17] suggesting the occurrence of heavy metal migration and transformation during the combustion process, complicating the management of heavy metal volatilization.[18] Presently, the primary solution to heavy metal volatilization involves the use of solid additives to capture or solidify the metals. Studies

Table 1. Ultimate and Proximate Analyses of Sewage Sludge[a]

	proximate analysis wt %				ultimate analysis wt %					
sample	M	V	A	FC	C	H	O	S	N	Q/kJ·kg^{-1}
Sludge A	53.16	43.70	47.75	8.55	17.88	4.95	25.15	0.74	3.53	8604
Sludge B	51.14	28.28	66.94	4.78	7.56	4.42	15.59	3.98	1.51	2579
Coal 1	2.09	29.44	11.81	56.66	68.93	3.78	13.87	0.62	0.99	23,180
Coal 2	8.07	42.05	7.8	42.08	60.06	4.04	26.72	0.50	0.88	17,160
Coal 3	1.89	31.37	16.88	50.60	64.51	3.92	12.84	0.77	1.08	24,090
Coal 4	2.16	29.35	17.09	51.40	63.65	3.65	13.92	0.70	0.99	21,830

[a]M: moisture (wt %) (as received), V: volatile matter (wt %) (dried basis), A: (wt %) (dried basis), FC: fixed carbon (wt %) (dried basis).

have shown that additives such as limestone, alumina, and kaolin effectively remove heavy metal vapors from the flue gas when added to the sludge.[19,20] Furthermore, coal addition to sludge contributes to the solidification of heavy metals in the resulting combustion ash.[21,22] However, although the individual utilization of coal and sludge is associated with some challenges, their co-combustion may present a new practical solution. Nonetheless, maintaining an appropriate reaction temperature remains key to successful co-combustion.

A desirable combustion process needs to be energy-conserved and have low emissions. The ash melting behavior attracts serious consideration during the combustion process as it leads to issues such as fouling and slagging and affects the safety and stability of the process. Regarding the sludge combustion processes, fluidized bed combustion is one of the most attractive methods for sludge utilization.[23,24] The fluidized bed combustion has advantages in low-rank solid fuel (sludge) combustion in an energy conservation and environmentally friendly manner. The ash fusion temperature is an important indicator for furnace and combustion process design. The ash fusion process is divided into three stages: mineral transformation, formation of the initial liquid phase, and melting of the residual solid phase.[25,26] Incinerator selection based on the melting properties of the sludge is critical for the sludge combustion process.[27] Particles with relatively low-melt viscosity are prone to slag formation.[28] Furthermore, slag viscosity is a critical melting property that has a significant impact on glass production, metallurgical processes, fly ash vitrification, combustion, and gasification.[29,30]

Otero et al. analyzed the thermal degradation of coal, urban sewage sludge, and their four blends through nonisothermal isoconversional methods proposed by Ozawa, Flynn, Wall, and Vyazovkin.[31] Their study found that the activation energy of coal combustion was lower than that of sewage sludge combustion. The activation energy of the coal-sludge blend was close to that of coal alone, and the difference in combustion between coal and sludge was weakened owing to their co-combustion. Wang et al. investigated the co-combustion of lignite and waste-activated sludge and proved that the high concentration of oxygen increased the volatility of trace elements.[32] Chen et al. investigated the differences between sludge combustion and sludge−coal co-combustion and the changes in trace elements and pollutant gases.[33] The presence of coal accelerated sludge combustion and reduced the emissions of gases, such as SO_2, CH_4S, and COS. Furthermore, it stabilized trace elements, such as Cd and Pb, in low-impurity slag. Lv et al. investigated methods for reducing the emission of nitrogen oxides during the co-combustion of coal and sludge.[34] High-temperature preheating technology was applied to facilitate the conversion of nitrogen

in the fuel to nitrogen gas. Qi et al. investigated the co-combustion of Quandong coal and sludge and found that sodium catalyzed and improved the combustion performance of sludge and coal.[35] Moreover, the results revealed that sludge and coal were more likely to produce slag at a combustion temperature above 900 °C.

The current research on the ash characteristics of sludge and coal co-combustion mainly focuses on the study of Na and heavy metals. Their ash melting characteristics are mainly reflected in the change of the ash melting point, which is only the most basic research. The change in the ash melting point is only a characterization of ash melting. Therefore, no one has studied the flow characteristics of ash under high-temperature conditions. The synergistic effect of the ash components of sludge and coal on their flow characteristics under high-temperature conditions has not been investigated in the literature.

In this study, the ash melting behaviors for the sludge/coal co-combustion are explored by experimental and thermodynamic approaches. The mobility of the coal-mixed sludge is examined by the modified inclined plane method, where the key factors, including the basicity of the ash and the typical alkaline elements (CaO and Fe_2O_3) that affect the slag flowability, have been clarified at high temperatures. It is expected to provide valuable reference for the implementation of sludge incineration processes in sewage treatment plants.

2. EXPERIMENTAL SECTION

2.1. Sewage Sludge Preparation. Sludge A and Sludge B were collected from two sewage treatment plants in Shanghai, China. Coal 1 and Coal 4 were obtained from a coal mine in Shan Xi Province, Coal 2 was obtained as brown coal from Indonesia, and Coal 3 was sampled from Mongolia. These samples were ground to a particle size of <200 μm. The ash composition was analyzed by using an ARL-9800 X-ray fluorescence. A Rigaku SmartLab X-ray diffractometer was employed for ash-crystallized phase characterization. The test conditions were a tube voltage of 40 kV and 40 mA. SEM-EDS was performed by using a Japanese electronic JSM-6390A scanning electron microscope with a voltage of 15 kV, and the sample surface was treated with gold spray. The proximate and ultimate analysis results are listed in Table 1. The slag fluidity experiment was conducted in a horizontal furnace through the modified inclined plane (M-IP) method, which had been previously employed in a study on coal fluidity. For each sample, 200 mg of ash was selected and formed into a material measuring 10 × 10 × 2 mm, without the addition of any viscous materials. The material was placed on a 50 × 20 × 2 mm aluminum plate. The sample was placed at an angle of 25°,

which was aligned with the angle of the refractory wall in the furnace.

The moisture contents of Sludge A and Sludge B exceeded 50%, with a low carbon content, which resulted in high energy consumption upon direct incineration. Therefore, co-combustion with other fuels is essential. Sludge A and Sludge B possessed a high oxygen content and a low sulfur content, making them suitable for incineration, as they yield less SO_2 during combustion.[36] However, determining the optimal mixing ratio of sludge and coal for combustion is essential and warrants further research. The optimal mixing ratio reduces the amount of coal required for sludge combustion, reduces slag formation, prolongs the service life of the incinerators, and improves sludge treatment efficiency.

The ash was obtained by ashing the sludge and coal samples following the national standard GB/T 1574-2007.[37] The experimental design and procedures were described in our previous studies.[29,30] Table 2 presents the chemical composi-

Table 2. Ash Compositions of Sewage Sludges and Coals

	Sludge A	Sludge B	Coal 1	Coal 2	Coal 3	Coal 4
CaO	9.56	12.70	31.6	12.1	12.1	21.2
Fe_2O_3	12.83	45.29	5.9	20.0	1.8	5.5
Al_2O_3	13.35	5.29	20.8	22.1	50.3	32.6
SiO_2	20.95	11.79	25.9	28.0	25.5	24.9
P_2O_5	32.44	2.02	0	0	0.5	0
TiO_2	1.25	2.21	0.8	0.7	2.6	2.3
K_2O	3.43	1.01	1.1	1.2	0.3	1.4
Na_2O	0	0	1.6	0	0	1.6
MgO	0	0	3.5	5.3	0	2.3
SO_3	4.91	18.31	8.6	10.0	6.8	8.2
MnO	0.18	0.22	0	0.5	0	0
base/acid	0.73	3.06	0.92	0.76	0.18	0.54

tions of two types of sludge and four types of coal. The base/acid ratios of Sludge A and Sludge B differed significantly. Sludge A exhibited a stronger acidity with a base/acid ratio of 0.73, whereas Sludge B exhibited a stronger alkalinity, with a base/acid ratio of 3.06. Sludge B was mixed with Coal 3 and Coal 4 in certain mass percentages to form samples with different base/acid ratios.

Coal 1 presented a higher CaO content (31.6%) than the other three coal samples, whereas Coal 2 exhibited a higher Fe_2O_3 content (20%) than the other three samples. To study the effect of the CaO and Fe_2O_3 contents of the sludge on the sludge fluidity properties, Sludge A was mixed with Coal 1 in varying mass percentages to form ash samples. Sludge A was also mixed with Coal 2 at different mass percentages to form ash samples, and the effect of Fe_2O_3 on the sludge fluidity properties was studied.

2.2. Ash Fusion Temperature Test. The AFTs of ash with sludges and coals were measured under a CO/CO_2 (6:4, volume fraction) atmosphere according to the Chinese standard GB/T 219-2008. The ash cone was heated to 900 °C at 15 °C·min^{-1} and then increased at 5 °C·min^{-1} to the flow temperature (FT). Four characteristic temperatures were recorded: deformation temperature (DT), softening temperature (ST), hemispherical temperature (HT), and FT.

2.3. Thermodynamic Equilibrium Calculation. FactSage is an integrated thermochemical data-bank system consisting of a suite of information, database, and calculation modules.[38,39] The Equilib module is one of the main components in FactSage and is widely utilized due to its ability to calculate concentrations of species in chemical reactions, particularly when equilibrium is reached. It is considered essential due to its comparatively low Gibbs free energy and high usage frequency. The Equilib module in FactSage 7.2 was used to assess the variation of the ash melting propensity of ash with its composition.[40,41] Equilib determines the combination of n_i, P_i, and X_i, which minimizes the total Gibbs energy G of the system in eq 1. For each calculation, the input included ash compositions, flue gas composition, and the products to be predicted, including real gases, pure liquid, pure solid, and solid solution database FT oxid-slag.

$$G = \sum_{\substack{\text{ideal} \\ \text{gas}}} n_i(g_i^0 + RT \ln P_i) + \sum_{\substack{\text{pure} \\ \text{condensed} \\ \text{phases}}} n_i g_i^0$$

$$+ \sum_{\text{solution}-1} n_i(g_i^0 + RT \ln X_i + RT \ln \gamma_i)$$

$$+ \sum_{\text{solution}-2} n_i(g_i^0 + RT \ln X_i + RT \ln \gamma_i)$$

$$+ \sum_{\text{solution}-n} n_i(g_i^0 + RT \ln X_i + RT \ln \gamma_i) \tag{1}$$

where n_i is the moles, P_i is the gas partial pressure, X_i is the mole fraction, γ_i is the activity coefficient, g_i^0 is the standard molar Gibbs energy, and i is the chemical composition of in the reaction system, CaO, Fe_2O_3,....SO_3, M_nO.

3. RESULTS AND DISCUSSION

3.1. Melting Temperatures of Sludge and Coal. When co-combusting sludge and coal, several processes take place at
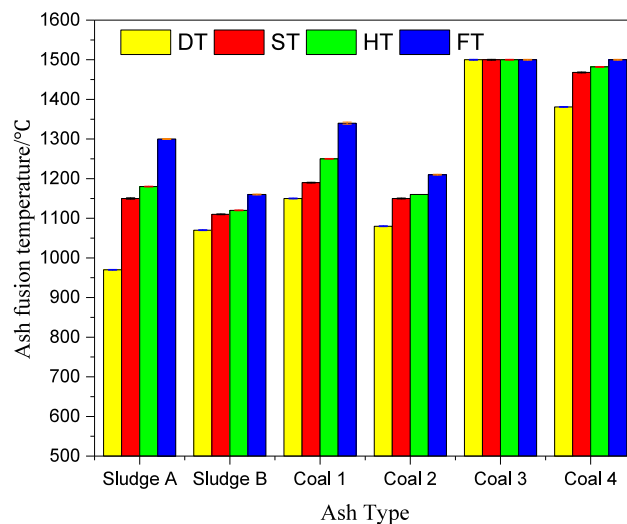
Figure 1. Ash fusion temperatures measured for the four ashes under the GB/T 219-2008 standard. DT, ST, HT, and FT denote the deformation temperature, starting sphere temperature, hemispherical temperature, and fusion temperature, respectively.

different temperature ranges. Water loss occurs below 200 °C, organic and organic polymer decompositions occur at 200−400 °C, and nonbiodegradable organic matter decomposition occurs above 400 °C.[42] Figure 1 depicts the melting temperature of sludge and coal, tested in a reducing atmosphere (40% CO) according to the standard GB/T
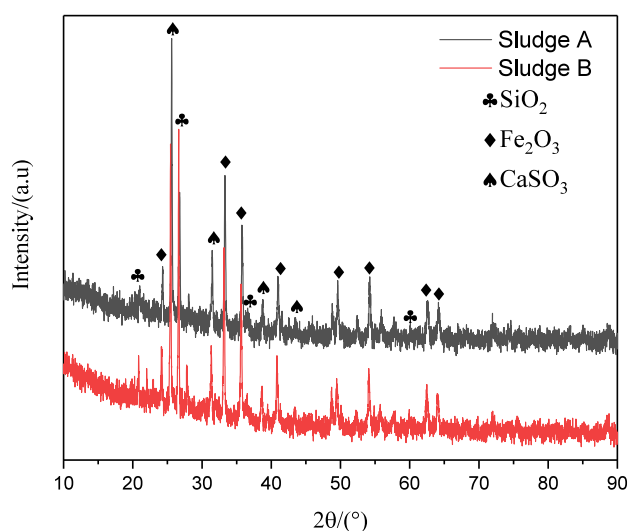
**Figure 2.** X-ray diffraction patterns of Sludge A and Sludge B.

219-2008. Sludge A, Sludge B, and Coal 2 exhibited low DTs and STs, both of which were lower than 1160 °C, indicating that they belonged to easy-to-melt ash. Coal 1 had an ST of 1190 °C and thus belonged to medium-melted ash. Therefore, its suitability needs to be considered during co-combustion with sludge. The ST temperature of Coal 3 exceeded 1500 °C, which indicates that it belonged to nonmelting ash. Therefore, during the co-combustion of sewage sludge with coal, considering the slagging temperature and the ash fusion characteristics of the sludge is vital. A higher ash fusion

temperature corresponds to a lower tendency of the sludge to form slag. Conversely, under a low ash fusion temperature, significant slag formation can occur. The inclusion of SiO_2 and CaO in sludge substantially enhanced its fusion temperature because CaO possesses an inherently high melting point, and SiO_2 acts as a solvent, facilitating the comelting of other oxides and raising the sludge's fusion temperature. Fe_2O_3 exhibited a specific mass fraction of 10−20%, under which the sludge exhibited its maximum crystallization temperature (DT). Furthermore, Fe_2O_3 reduced the sludge fusion temperature by inducing the formation of different iron forms at varying temperatures. Hence, as temperature increased, the formation of low-melting eutectic compounds decreased the sludge's fusion temperature. SiO_2 and CaO impeded the sludge transformation into a liquid at high temperatures, thereby elevating the FT. Conversely, at elevated temperatures, Fe_2O_3 reduced the sludge fusion temperature and enhanced the flowability during the melting process.

Figure 2 depicts the X-ray diffraction patterns of Sludge A and Sludge B. The major peaks observed in Sludge A and Sludge B corresponded to SiO_2, Fe_2O_3, and $CaSO_3$. The presence of SiO_2 and Fe_2O_3 increased the melting points of Sludge A and Sludge B, particularly for Sludge B, and DT, ST, HT, and FT exceeded 1000 °C. Figure 3 illustrates the melting temperature profile of the cofiring of Sludge A with Coal 1 and Coal 2 and the melting temperature profile of a mixture of Sludge B and Coal 3. In all cases, the addition of coal increased the melting temperature of the sludge. With the addition of Coal 1 to Sludge A at an increasing mass fraction from 40 to 80%, DT, ST, HT, and FT increased. The Sludge A−Coal 2
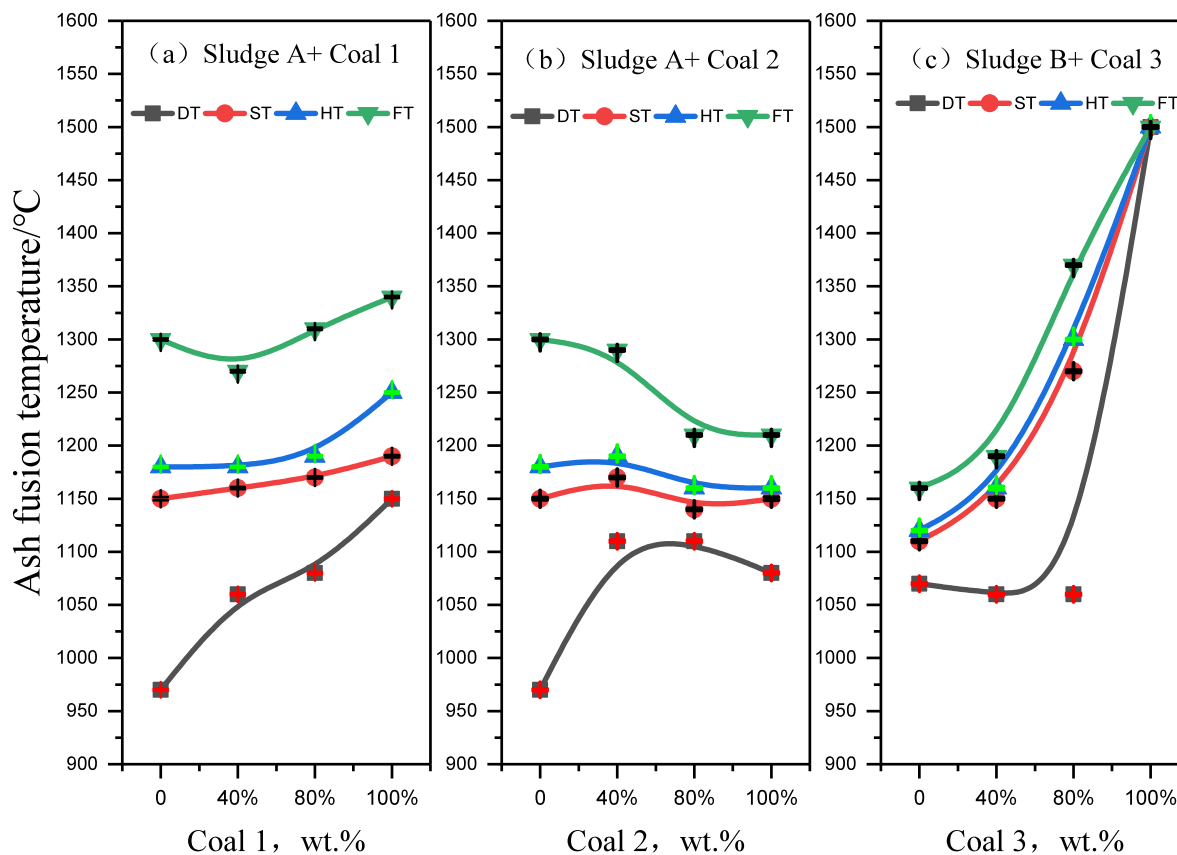
Figure 3. (a−c): Melting analysis results were of mixtures of Sludge A with Coal 1 and Coal 2 and Sludge B with Coal 3 at varying mass fractions.
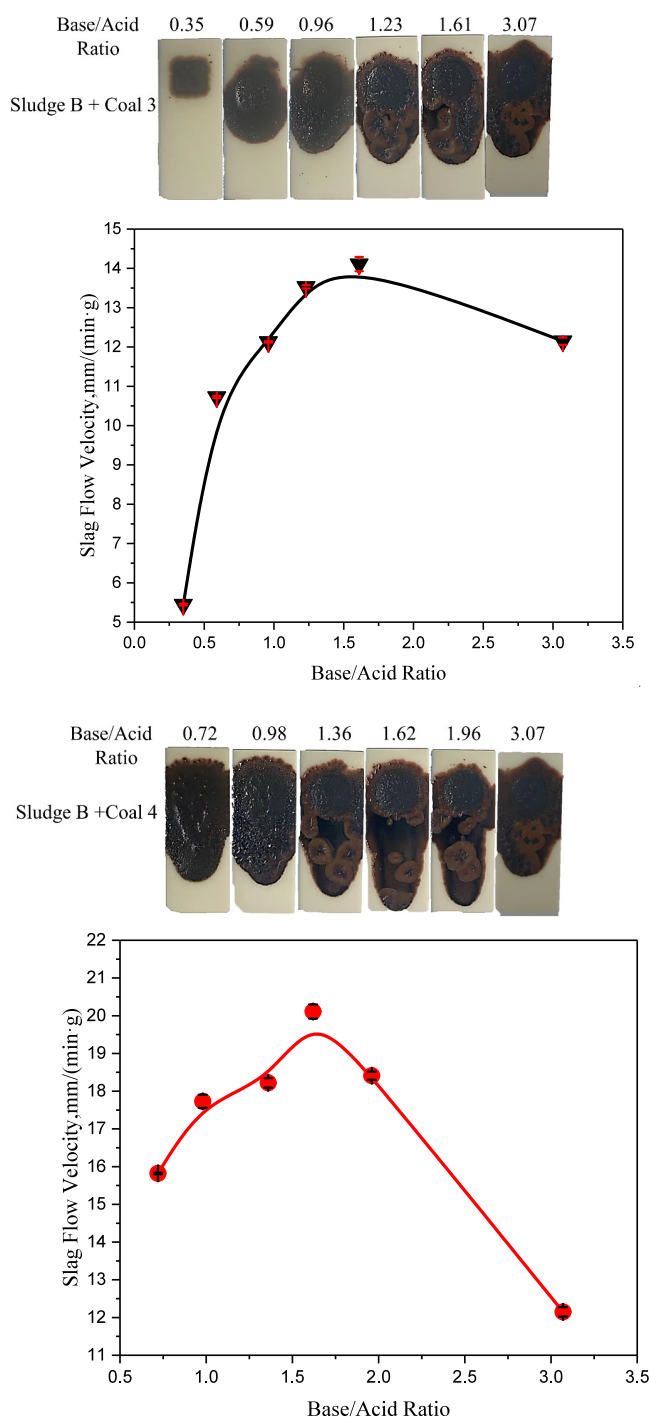
Figure 4. Fusion and flow characteristics of ashes produced by cofiring Sludge B with Coal 3 and Coal 4: the base/acid ratio range of Coal 3 and Coal 4 varied between 0.35 and 3.07 at a temperature of 1300 °C and an exposure time of 60 min.

mixture exhibited the highest melting temperature at a Coal 2 mass fraction of 40%, The melting point at a mass fraction of 80% was lower, mainly because of the increase in the SiO_2 mass fraction, which facilitated melting. Given that Coal 3 had a high Al_2O_3 content (50.3%), DT, ST, HT, and FT all exceeded 1500 °C. The addition of Coal 3 to Sludge B significantly increased its melting temperature. Therefore, considering the mass fractions of Al_2O_3 and SiO_2 in ash and coal, the determination of the optimal mass ratio for sludge and coal blending is vital to promote low slagging, facilitate the

disposal of incinerator ash, and ensure the efficient combustion of sludge using coal as fuel. The combination of sludge and coal with a low melting point and high fluidity is more suitable for co-combustion in incinerators.

3.2. Effect of Basicity on Sludge Ash Fluidity. The fluidity of sludge ash aluminum sheets was affected by the base/acid ratio. The base-to-acid ratio (base/acid) of the ash samples is calculated using eq 2 (all oxides of the ash are selected in the calculation except P_2O_5 and SO_3).[43]

$$\text{base/acid} = \frac{m_{Na_2O} + m_{K_2O} + m_{MgO} + m_{CaO} + m_{Fe_2O_3}}{m_{SiO_2} + m_{Al_2O_3}}$$

(2)

where m_i is the mass of chemical components in the reaction system and i are Na_2O, K_2O, MgO, CaO, Fe_2O_3, SiO_2, and Al_2O_3.

Therefore, Sludge B, Coal 3, and Coal 4 were mixed at sludge weight percentages of 80, 70, 60, 40, and 20% to produce ash samples. The range of the base/acid ratio was 0.35−3.07. The travel length of slag on the inclined plane follows an Arrhenius-type relationship, which is widely used to describe the temperature dependence of slag viscosity.[35,44] At a base/acid ratio of 1.62, the maximum flow velocity was 20.11 mm/(min·g). At a base/acid ratio of 0.35, the Sludge B−Coal 2 mixture exhibited a lower flow velocity of 5.45 mm/(min·g), which inhibited the flow of Sludge B on the aluminum plate. With an increasing base/acid ratio, the flow velocity of Sludge B on the aluminum plate first increased and then decreased. Thus, the optimal base/acid ratio was 1.61, and the maximum flow velocity was 14.11 mm/(min·g).

Fusion and flow characteristics of ashes produced by coal and sludge can be seen in Figure 4. When the mass fraction of Sludge B in the Sludge B−Coal 4 mixture samples was 70%, the base/acid ratio of the sludge was 1.62, and the flow distance of ash was the greatest. In the Sludge B−Coal 3 samples, when the mass fraction of Sludge B was 80%, its base/acid ratio was 1.61, and the flow distance of ash was the greatest. Therefore, a base/acid ratio existed that allowed the ash to flow on the aluminum plate at the highest speed. Overacidity or overalkalinity inhibits the flow of ash on the aluminum plate. A base/acid ratio of 1.6 maximized the flow velocity and flow distance of Sludge B on the aluminum plate.

To align with the experimental findings, thermodynamic calculations have been employed to clarify the ash transition route during high temperature under the equilibrium model. The ash compositions have been used as the input, and an oxidizing atmosphere composed has been applied in the calculations to maintain consistency with the experimental conditions. These calculations were performed in the temperature range from 90 to 1400 °C, and the gas pressure was kept at 1 atm. The figure on the left side of Figure 5 displays the actual flow of experimental ash on the aluminum sheet, and that on the right side displays the changes in the solid and liquid phase mass fractions, simulated by FactSage 7.2. The blue line on the graph represents the percentage of the liquid phase content, and the shaded area represents the range of the liquid phase. The different colors and sizes of the area denote the contents of the different solid components.

Sludge A and Sludge B were analyzed via the MIP method. The sludge was held at a high temperature for 1 h. At 1000 °C, the shape of Ash A's rectangular prism remained unchanged, but black spots melted into particles that appeared at the prism
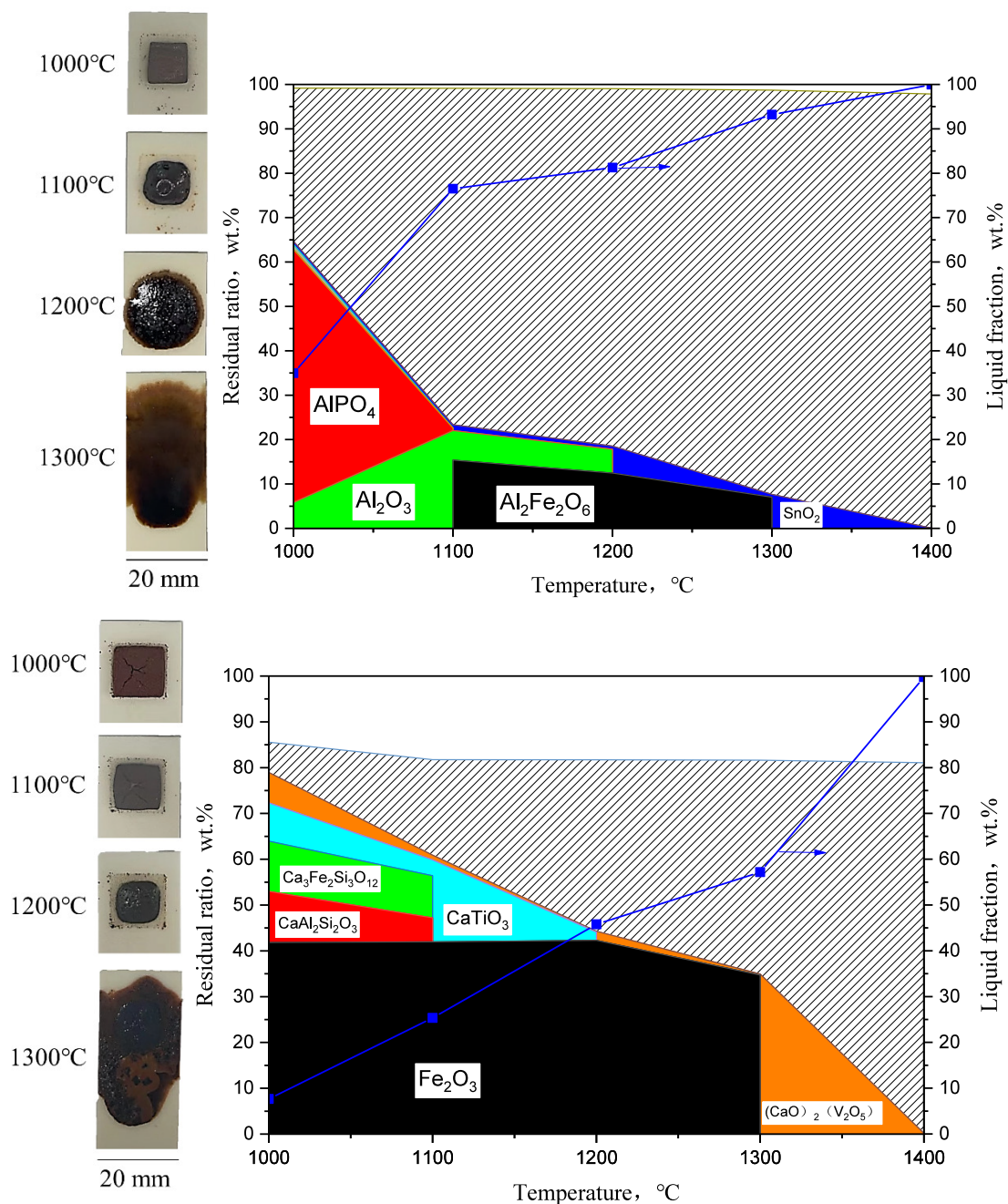
Figure 5. Ash melting and flowability for two raw sludges (A and B) at different temperatures. Solid phase melting analysis was performed using the Equilib module of FactSage 7.2.

edges. As the temperature gradually rose to 1100 and 1200 °C, the ash gradually turned black, indicating the occurrence of sintering. At 1200 °C, Ash A spread into a circular shape, indicating a significant degree of melting and sintering. Generally, from the optical macroscopy images, all the samples provide a shiny flat surface, indicating that the ash was fully melted with the molten phase.[45] Furthermore, the liquid phase content gradually increased to 80%. Although a high liquid phase content caused the ash to shrink, the solid:liquid ratio did not cause the ash to flow on the aluminum sheet. The high ratio of the liquid phase in suspension enhanced the fluidity of the slurry; however, the high ratio of the liquid phase was not the sole factor influencing the sludge flow on aluminum sheets.

Once the temperature rose to 1300 °C, the molten ash began to diffuse and flow on the alumina plate.

At 1000 °C, black spots appeared at the edges of the cube of Ash B, and unlike Ash A, the volume of Ash B did not shrink significantly because it was composed of solid phases less prone to melting, such as $CaAl_2Si_2O_3$ and $Ca_3Fe_2Si_3O_{12}$. When the melting point of the solid phase in Ash A was high, the solid phase component was not easily converted into the liquid phase. According to the FactSage 7.2 simulation results, the liquid phase content at this temperature was less than 10%. At 1200 °C, Ash B contracted into a smooth surface.[46] At a high temperature of 1300 °C, Ash B flowed on the aluminum sheet, but some solid components did not flow. At this time, the liquid phase content was 60% owing to the formation of
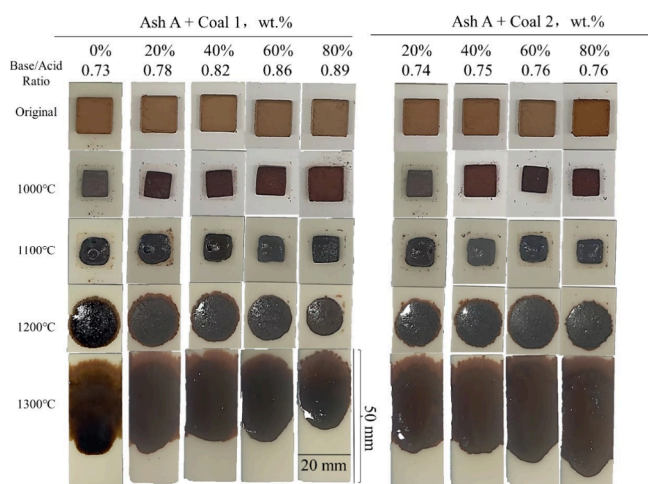
Figure 6. Ash melting and fluidity of basic Ash A blended with 20−80 wt % Coal 1 and Coal 2 at 1300 °C. The exposure time was 60 min.
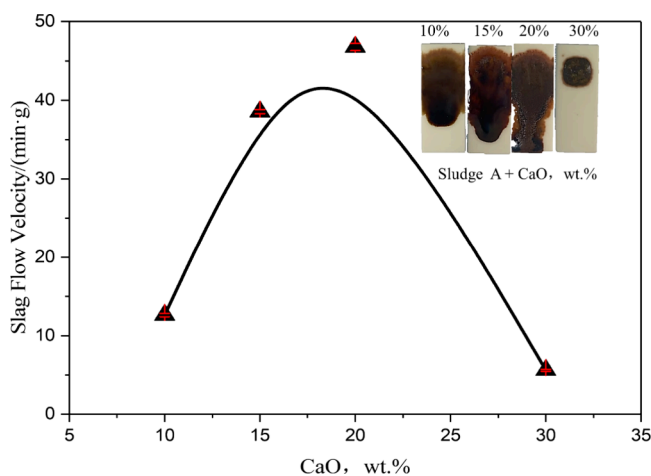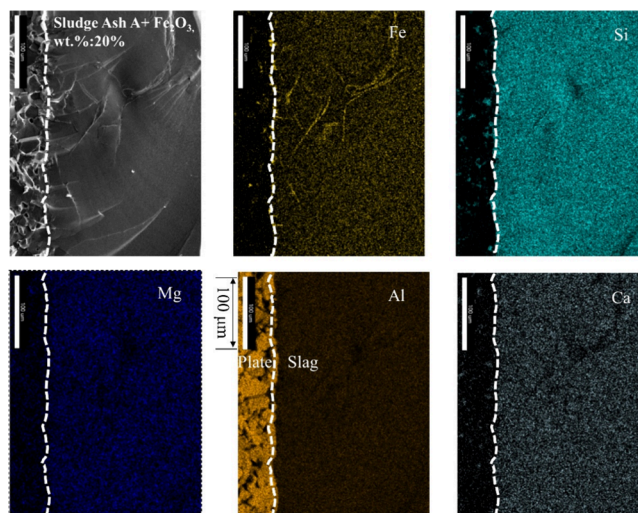

Figure 7. Melting and flow of Sludge A with a CaO content of 10−30% at a temperature of 1300 °C and an exposure time of 60 min.
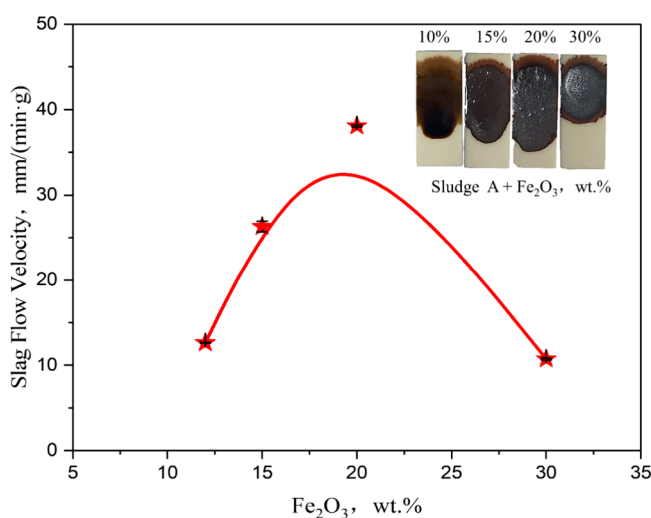
Figure 8. Variation in Sludge A flow velocity with an increasing Fe_2O_3 mass fraction.

Figure 9. Elemental mapping for the cross section of the corundum plate loaded with Sludge A + Fe_2O_3 (wt %:20%) at 1300 °C. The dashed curve refers to the interface between the liquid slag and corundum substrate.

under the current temperature conditions. However, the liquid phase content was not the only influencing factor. Ash flow was also related to the melting point of the constituent metal oxides. Hence, the CaO and Fe_2O_3 contents and base/acid ratio of the sludge influenced sludge flow on aluminum sheets.

As mentioned above, Coal 1 and Coal 2 contained higher CaO and Fe_2O_3 levels. By using X-ray fluorescence analysis, the CaO mass fraction of Coal 1 was determined to be 31.6%, while the Fe_2O_3 mass fraction of Coal 2 was found to be 20.0%. The next step is to calculate the required mass of Coal 1 and Coal 2 to achieve the desired CaO and Fe_2O_3 mass fractions in Sludge A. Once these masses are calculated, they will be added to Sludge A. To study the effects of CaO and Fe_2O_3 contents on ash fluidity, Sludge A was mixed with Coal 1 and Coal 2 at different mass ratios, as shown in Figure 6, where the percentages indicate the mass percentage of sludge. The base/acid ratios of the sludge and coal groups were similar to prevent the base/acid ratio from affecting the sludge flow. At 1000 °C, the samples of Sludge A mixed with Coal 1 and Coal 2 showed volume shrinkage compared to the original samples. At 1100 °C, Sludge A shrank and agglomerated into smooth surface lumps. At 1200 °C, both the Sludge A−Coal 1 and Sludge A−Coal 2 mixtures changed from a spread-out mass to a circular shape with reducing sludge mass percentage. At 1300 °C, mixing Sludge A with different ratios of Coal 1 and Coal 2 resulted in significantly different flow distances of Sludge A, indicating that CaO and Fe_2O_3 affected sludge flow.

3.3. Effect of CaO and Fe_2O_3 on Sludge Ash Fluidity. To quantify the effect of CaO and Fe_2O_3 on sludge ash fluidity, pure CaO and Fe_2O_3 were mixed with Sludge A, and the temperature was set to 1300 °C for 1 h. Sludge A samples were prepared with different mixing ratios, and the sludge flow distance per unit time and unit mass was defined as the melting flow rate. Sludge A samples doped with pure CaO and Fe_2O_3 reagents were analyzed. By using the ARL-9800 X-ray fluorescence analysis, the mass fraction of CaO in Sludge A was found to be 9.56% and the mass fraction of Fe_2O_3 was 12.83%. The author will now calculate the required mass of pure CaO and Fe_2O_3 for each sample and add them to Sludge A. The samples were divided into different groups based on

$(CaO)_2(V_2O_5)$, which had a high melting point and was not melted at 1300 °C. Therefore, the flow of Ash A and Ash B on aluminum sheets was influenced by the liquid phase content

CaO mass percentages of 10, 15, 20, and 30%. Sludge A flow on aluminum sheets at 1300 °C was observed. Figure 7 shows the flowchart of Sludge A with different CaO doping ratios. At a 10% mass fraction, Sludge A melted and flowed onto the aluminum sheet, forming a glassy state. FactSage 7.2 simulation results showed that the solid components $AlPO_4$, Al_2O_3, and $Al_2Fe_2O_6$ were melted. Increasing the mass fraction of CaO to 15% under the same experimental conditions resulted in an increase in the flow distance of Ash A. At a higher CaO mass fraction of 20%, the flow distance of Ash A significantly increased, with the ash reaching the edge of the aluminum sheet. However, with a further increase in the CaO mass fraction to 30%, Ash A contracted to a circular shape and did not flow. Therefore, 20% was the optimal CaO mass fraction to promote the Ash A flow.

When the mass fraction of CaO in Sludge A was 10%, the flow velocity of Ash A was 12.63 mm/(min·g). At a higher CaO mass fraction of 20%, the flow velocity of Ash A reached 46.8 mm/(min·g). CaO exhibited the optimal promoting effect on the flowability of Sludge A at a 20% mass fraction and base/acid ratio of below 1.

With increasing Fe_2O_3 content in Sludge A, the flow distance of Ash A increased, as shown in Figure 8. At a 20% Fe_2O_3 content, the flow distance of Ash A was the greatest. When the Fe_2O_3 mass fraction of Sludge A increased from 10 to 15%, the flow velocity of Ash A increased to 23.6 mm/(min·g). Furthermore, the presence of Fe_2O_3 promoted the flowability of Sludge A. At 20% Fe_2O_3, the flow velocity of Ash A was 38.1 mm/(min·g). A comparison of the flow rates of Sludge A revealed the promoting effects of CaO and Fe_2O_3 on the ash flow rate. Therefore, 20% was the optimal Fe_2O_3 mass fraction to promote Sludge A flowability.

The sample preparation involved cutting transverse sections of aluminum sheets coated with Sludge A, which contained 20% Fe_2O_3, at the bottom of the sludge-covered aluminum sheets. The scanning electron microscopy image of the transverse section of Sludge A is presented in Figure 9, where the left side of the white line corresponds to aluminum, and the right side represents the microstructure of Sludge A. The image reveals a highly polished surface of the sample, attributed to the slow motion of the flowing material at high temperatures. Fe, Ca, and Mg ions occurred at the end of the ash flow, indicating that they coflowed with the molten liquid in the melting process at high temperatures, without any noticeable accumulation in the middle of the sludge. Moreover, the aluminum sheet at the left of the white line shows the presence of Fe and Ca ions, suggesting that both ions penetrated the surface of the aluminum sheet and migrated into its interior while the sheet was tilted. This demonstrates the strong penetration ability of metal ions.

4. CONCLUSIONS

The melting behavior and the flowability of ash for the co-combustion of sludge and coal at high temperature were investigated through experimental and thermodynamical approaches. The synergistic interaction for ash-forming metals was clarified, and the key factors that affect the flow ability were explored. It has been confirmed that the high melting point of CaO and the cosolvent effect of SiO_2 increase the melting point of the sludge, while the presence of Fe_2O_3 reduces the melting point of the sludge. Due to the interaction of ash-forming metals, the slag flow ability is maximized at a base/acid ratio of 1.6. The coexistence of Fe/Ca/Si promotes

the melting behavior and fluidity due to the synergistic reaction, where Fe and Mg indicate an initial melting tendency due to the precipitation. The findings are expected to provide reference for the selection of combustion process for the thermal treatment of sludge.

■ AUTHOR INFORMATION

Corresponding Author

Baiqian Dai − *Department of Chemical&Biological Engineering, Monash University, Clayton, Victoria 3800, Australia; Monash Suzhou Research Institute, Suzhou, Jiangsu 215028, China;* ⓘ orcid.org/0000-0001-6741-0985; Email: Bai-qian.Dai@monash.edu

Authors

Yunpeng Yu − *Department of Chemical&Biological Engineering, Monash University, Clayton, Victoria 3800, Australia; Monash Suzhou Research Institute, Suzhou, Jiangsu 215028, China*

Zhiao Yu − *School of Software Engineering, Southeast University, Suzhou 215723, China*

Wei Xu − *General Water of China Co., Ltd., Beijing 100022, China*

Kaibing Zhang − *Department of Chemical Engineering, Southeast-Monash Joint Graduate School, Suzhou 215123, China*

Yuneng Tang − *Department of Chemical&Biological Engineering, Monash University, Clayton, Victoria 3800, Australia; Monash Suzhou Research Institute, Suzhou, Jiangsu 215028, China*

Guojian Cheng − *JITRI Institute for Process Modeling and Optimization, Suzhou 215123, China*

Xiang He − *University of Shanghai for Science and Technology, Shanghai 200093, China; Shanghai Power Equipment Research Institute Co.,Ltd., Shanghai 200240, China*

Complete contact information is available at:
https://pubs.acs.org/10.1021/acsomega.4c00227

Notes

The authors declare no competing financial interest.

■ REFERENCES

(1) Salado, R.; Vencovsky, D.; Daly, E.; Zamparutti, T.; Palfrey, R. Environmental, economic and social impacts of the use of sewage sludge on land Final Report Part I: Overview Report. 2010.

(2) Fu, J.; Yan, B.; Gui, S.; Fu, Y.; Xia, S. Anaerobic co-digestion of thermo-alkaline pretreated microalgae and sewage sludge: Methane potential and microbial community. *Journal of Environmental Sciences* **2023**, *127*, 133−142.

(3) Yan, Y.; Liu, F.; Gao, J.; Wan, J.; Ding, J.; Li, T. Enhancing enzyme activity via low-intensity ultrasound for protein extraction from excess sludge. *Chemosphere* **2022**, *303*, No. 134936.

(4) Ellersdorfer, M. Hydrothermal co-liquefaction of chlorella vulgaris with food processing residues, green waste and sewage sludge. *Biomass & bioenergy* **2020**, *142*, No. 105796.

(5) Werle, S.; Wilk, R. K. A review of methods for the thermal utilization of sewage sludge: The Polish perspective. *Renewable Energy* **2010**, *35* (9), 1914−1919.

(6) Folgueras, M. B.; Díaz, R. M.; Xiberta, J.; Prieto, I. Thermogravimetric analysis of the co-combustion of coal and sewage sludge. *Fuel* **2003**, *82* (15−17), 2051−2055.

(7) Font, R.; Fullana, A.; Conesa, J.; Llavador, F. Analysis of the pyrolysis and combustion of different sewage sludges by TG. *Journal of Analytical and Applied Pyrolysis* **2001**, *58*, 927−941.

(8) Fytili, D.; Zabaniotou, A. Utilization of sewage sludge in EU application of old and new methods—A review. *Renewable and sustainable energy reviews* **2008**, *12* (1), 116−140.

(9) Solimene, R.; Urciuolo, M.; Cammarota, A.; Chirone, R.; Salatino, P.; Damonte, G.; Donati, C.; Puglisi, G. Devolatilization and ash comminution of two different sewage sludges under fluidized bed combustion conditions. *Experimental thermal and fluid science* **2010**, *34* (3), 387−395.

(10) Kijo-Kleczkowska, A.; Środa, K.; Kosowska-Golachowska, M.; Musiał, T.; Wolski, K. Experimental research of sewage sludge with coal and biomass co-combustion, in pellet form. *Waste Manag.* **2016**, *53* (jul.), 165−181.

(11) Nadziakiewicz, J.; Kozioł, M Co-combustion of sludge with coal. *Applied Energy* **2003**, 239 DOI: 10.1016/S0306-2619(03)00037-0.

(12) Abbas, A. H.; Aris, M. S.; Sulaiman, S. A.; Fadhil, M.; Karuppanan, S.; Abdul Karim, Z. A.; Ovinis, M.; Tesfamichael Baheta, A. A Non-isothermal Thermogravimetric Kinetic Analysis of Malaysian Sewage Sludge. *MATEC Web Conf.* **2014**, *13*, No. 06012.

(13) Wang, R.; Zhao, Z.; Qiu, L.; Liu, J. Experimental investigation of synergistic behaviors of lignite and wasted activated sludge during their co-combustion. *Fuel Process. Technol.* **2017**, S037838201630491X.

(14) Niu, H.; Li, S.; Shen, J.; Yao, M. Characteristics of heavy metal accumulation on fly ash- and sewage sludge-amended calcific soil. *Chin. J. Geochem.* **2012**, 181 DOI: 10.1007/s11631-012-0565-3.

(15) Helena Lopes, M.; Abelha, P.; Lapa, N.; Oliveira, J. S.; Cabrita, I.; Gulyurtlu, I. The behaviour of ashes and heavy metals during the co-combustion of sewage sludges in a fluidised bed. *Waste Manag.* **2003**, *23* (9), 859−870.

(16) Gorazda, K.; Kowalski, Z.; Wzorek, Z.; Jodko, M.; Rzepecki, T.; Kulczycka, J.; Przewrocki, P. Possibilities of phosphorus recovering from municipal sewage and sewage sludge. *Pol. J. Appl. Chem.* **2003**, 51.

(17) Tian, S.; Chen, J.; Yan, F.; Lang, C.; Strezov, V.; Zhang, Z. Cross-sectoral synergy between municipal wastewater treatment, cement manufacture and petrochemical synthesis via clean transformation of sewage sludge. *Sustainable Energy Fuels* **2020**, *4*, 6274 DOI: 10.1039/D0SE01164A.

(18) Ren, Q.; Li, L. Co-combustion of Agricultural Straw with Municipal Sewage Sludge in a Fluidized Bed: Role of Phosphorus in Potassium Behavior. *Energy Fuels* **2015**, *29* (jul.-aug.), 150610080748000.

(19) Yu, S.; Zhang, B.; Wei, J.; Zhang, T.; Yu, Q.; Zhang, W. Effects of chlorine on the volatilization of heavy metals during the co-combustion of sewage sludge. *Waste Manag.* **2017**, *62*, 204−210.

(20) Jang, J. G.; Kim, M. R.; Kim, W. H.; Lee, J. K. Effect of Cl/S molar ratio on theoretical partitioning of heavy metals under waste combustion conditions. *Korean Journal of Chemical Engineering* **2002**, *19* (6), 1097−1105.

(21) Wang, K. S.; Chiang, K. Y.; Tsai, C. C.; Sun, C. J.; Tsai, C. C.; Lin, K. L. The effects of FeCl3 on the distribution of the heavy metals Cd, Cu, Cr, and Zn in a simulated multimetal incineration system. *Environ. Int.* **2001**, *26* (4), 257−263.

(22) Liu, J.; Zeng, J.; Sun, S.; Huang, S.; Kuo, J.; Chen, N. Combined effects of FeCl3 and CaO conditioning on SO2, HCl and heavy metals emissions during the DDSS incineration. *Chemical Engineering Journal* **2016**, *299*, 449−458.

(23) Van Caneghem, J.; Brems, A.; Lievens, P.; Block, C.; Billen, P.; Vermeulen, I.; Dewil, R.; Baeyens, J.; Vandecasteele, C. Fluidized bed waste incinerators: Design, operational and environmental issues. *Prog. Energy Combust. Sci.* **2012**, *38* (4), 551−582.

(24) Han, X.; Niu, M.; Jiang, X.; Liu, J. Combustion characteristics of sewage sludge in a fluidized bed. *Ind. Eng. Chem. Res.* **2012**, *51* (32), 10565−10570.

(25) He, C.; Bai, J.; Ilyushechkin, A.; Zhao, H.; Kong, L.; Li, H.; Bai, Z.; Guo, Z.; Li, W. Effect of chemical composition on the fusion behaviour of synthetic high-iron coal ash. *Fuel* **2019**, *253*, 1465−1472.

(26) Shi, W.; Bai, J.; Kong, L.; Li, H.; Bai, Z.; Vassilev, S. V.; Li, W. An overview of the coal ash transition process from solid to slag. *Fuel* **2021**, *287*, No. 119537.

(27) Wei, B.; Wang, X.; Tan, H.; Zhang, L.; Wang, Y.; Wang, Z. Effect of silicon−aluminum additives on ash fusion and ash mineral conversion of Xinjiang high-sodium coal. *Fuel* **2016**, *181*, 1224−1229.

(28) Juniper, L.; Creelman, R.; Ward, C.; Schumacher, G. Tools for evaluating slagging in boiler furnaces. In *Proceedings of the 22nd International Conference on Impacts of Fuel Quality on Power Production*, 2012.

(29) Ji, H.; Wu, X.; Dai, B.; Zhang, L. Xinjiang lignite ash slagging and flow under the weak reducing environment at 1300° C−Release of sodium out of slag and its modelling from the mass transfer perspective. *Fuel Process. Technol.* **2018**, *170*, 32−43.

(30) Wu, X.; Ji, H.; Dai, B.; Zhang, L. Xinjiang lignite ash slagging and flowability under the weak reducing environment at 1300° C−A new method to quantify slag flow velocity and its correlation with slag properties. *Fuel Process. Technol.* **2018**, *171*, 173−182.

(31) Otero, M.; Calvo, L.; Gil, M.; García, A.; Morán, A. Co-combustion of different sewage sludge and coal: a non-isothermal thermogravimetric kinetic analysis. *Bioresour. Technol.* **2008**, *99* (14), 6311−6319.

(32) Wang, R.; Zhao, Z.; Yin, Q.; Liu, J. Mineral transformation and emission behaviors of Cd, Cr, Ni, Pb and Zn during the co-combustion of dried waste activated sludge and lignite. *Fuel* **2017**, *199*, 578−586.

(33) Chen, J.; Sun, Y.; Zhang, Z. Evolution of trace elements and polluting gases toward clean co-combustion of coal and sewage sludge. *Fuel* **2020**, *280*, No. 118685.

(34) Lv, Z.; Xiong, X.; Ruan, R.; Wang, Y.; Tan, H. NO emission and burnout characteristics in co-combustion of coal and sewage sludge following high-temperature preheating. *Fuel* **2023**, *331*, No. 125887.

(35) Qi, X.; Song, G.; Song, W.; Yang, S.; Lu, Q. Combustion performance and slagging characteristics during co-combustion of Zhundong coal and sludge. *Journal of the Energy Institute* **2018**, *91* (3), 397−410.

(36) Zhou, L.; Jiang, X.; Liu, J. Characteristics of oily sludge combustion in circulating fluidized beds. *Journal of hazardous materials* **2009**, *170* (1), 175−179.

(37) Committee, C. N. S. M. *GBT1574−2007, Test Method for Analysis of Coal Ash*. Standard Press of China: Beijing, China, 2008.

(38) Eriksson, G.; Königsberger, E. FactSage and ChemApp: Two tools for the prediction of multiphase chemical equilibria in solutions. *Pure Appl. Chem.* **2008**, *80* (6), 1293−1302.

(39) Zhang, S.; Jiang, X.; Lv, G.; Nixiang, A.; Jin, Y.; Yan, J.; Lin, X.; Song, H.; Cao, J. Effect of chlorine, sulfur, moisture and ash content on the partitioning of As, Cr, Cu, Mn, Ni and Pb during bituminous coal and pickling sludge co-combustion. *Fuel* **2019**, 601 DOI: 10.1016/j.fuel.2018.11.061.

(40) Plaza, P.; Ferens, W.; Griffiths, A.; Syred, N.; Rybak, W. Predicting slagging/fouling propensities of solid fuels with the aid of experimental and modelling techniques. *Arch. Combust.* **2010**, *30* (3), 203−213.

(41) Jak, E.; Saulov, D. *Prediction of ash phase equilibria using FACT models*; Cooperative Research Centre for Coal in Sustainable Development 2005.

(42) Hernández, A. B.; Okonta, F.; Freeman, N. Thermal decomposition of sewage sludge under N 2, CO 2 and air: Gas characterization and kinetic analysis. *J. Environ. Manag.* **2017**, *196*, 560−568.

(43) Reinmoeller, E. M.; Bernd. Analysis and prediction of slag-induced corrosion of chromium oxide-free refractory materials during fusion of coal and biomass ash under simulated gasification conditions. *Fuel Process. Technol.* **2016**, *149* (Null), 218 DOI: 10.1016/j.fuproc.2016.04.022.

(44) Dai, B.; Wu, X.; Zhang, L. Establishing a novel and yet simple methodology based on the use of modified inclined plane (M-IP) for high-temperature slag viscosity measurement. *Fuel* **2018**, *233* (DEC.1), 299−308.

(45) Ji, H.; Zhou, Y.; He, Z.; Wu, X.; Dai, B. Bio-Slag High-Temperature Corrosion on an Alumina Refractory under the Reducing Environment. *Energy Fuels* **2021**, *35* (5), 3867 DOI: 10.1021/acs.energyfuels.0c03972.

(46) Wang, P.; Massoudi, M. Slag behavior in gasifiers. Part I: Influence of coal properties and gasification conditions. *Energies* **2013**, *6* (2), 784−806.